

Impact of solar wind disappearance event on Martian nightside ionospheric species: First results

L. Ram¹, D. Rout³, S. Sarkhel^{1, 2,*}

*Sumanta Sarkhel, Department of Physics, Indian Institute of Technology Roorkee, Roorkee - 247667, Uttarakhand, India (sarkhel@ph.iitr.ac.in)

¹Department of Physics,
Indian Institute of Technology Roorkee,
Roorkee - 247667
Uttarakhand, India

²Centre for Space Science and Technology,
Indian Institute of Technology Roorkee,
Roorkee - 247667
Uttarakhand, India

³National Atmospheric Research Laboratory,
Gadanki, India

Abstract

For the first time, we report the impact of a rarest solar wind phenomenon, i.e., disappearing solar wind (DSW) event on the Martian nightside ionosphere using MAVEN spacecraft datasets. During an extremely low solar wind density event, the nightside ionospheric densities particularly above 200 km, including electrons and ions (NO^+ , O_2^+ , CO_2^+ , C^+ , N^+ , O^+ , and OH^+) experience significant enhancement at a fixed altitude. The electron and ion densities increase by a factor of ~ 2.5 and $10\text{-}67$, respectively, compared to average quiet time. The increased plasma density, during DSW, suggests the expansion of the Martian ionosphere under extremely low solar wind dynamic pressure ($\sim 1.4 \times 10^{-11}$ Pa) contrasting with nightside ionospheric thermal pressure ($> 10^{-10}$ Pa). Further, the day-to-night plasma transport through cross-terminator magnetic topology may also be a contributing factor, causing the increased nightside ionospheric density. Therefore, this study sheds light on an unusual extreme state of the Mars-solar wind interaction.

Keywords: Mars-solar wind interaction, MAVEN, Disappearing solar wind (DSW), Martian nightside ionosphere.

Key Points:

- A noticeable increase in the Martian nightside ionospheric electron and ion density has been observed during the solar wind disappearance event.
- At fixed altitude, both electron and ion density increase by a factor of ~ 2.5 and $10\text{-}67$, respectively, compared to the average quiet time.
- The increased plasma density attributed to extreme low dynamic pressure compared to higher ionospheric thermal pressure in the nightside.

Plain Language Summary

The solar wind-Mars interactions have played a pivotal role in the evolution of Mars climate over time. Apart from Earth, there is a vague understanding of the influence of solar wind disappearance event on the planetary atmosphere/ionosphere especially on Mars, our neighboring planet. During the solar wind disappearance event, the top nightside ionosphere (~250-280 km altitudes) density increases as compared to pre- and post-event periods. Overall, at a fixed altitude, it is ~2.5 (for electrons) and 10-67 times (for ions) higher in magnitude compared to average quiet-time. The increased plasma density at a fixed altitude indicates the expansion of the Martian nightside ionosphere under low solar wind dynamic pressure ($\sim 1.4 \times 10^{-11}$ Pa) compared to higher nightside ionospheric thermal pressure ($> 10^{-10}$ Pa) during solar wind disappearance. Also, the IMF and day-to-night plasma transport via cross-terminator magnetic lines may be an additional factor for increased density in the nighttime ionosphere. In this letter, we reported, for the first time, the Martian nightside ionosphere response to the solar wind disappearance event. Hence, this study guides us to a new understanding of the impact of an end-member case of solar wind phenomena on planetary atmosphere/ionosphere in/out of our solar system for future exploration missions.

1. Introduction

The solar wind, originating from the solar corona, extends radially outward throughout our solar system, carrying the interplanetary magnetic field (IMF) within its flow. As it travels in space, the solar wind interacts with various celestial bodies, including planets, moons, asteroids, and comets. The nature of this interaction is primarily influenced by the intrinsic magnetic field and the atmospheric conditions of these bodies. For instance, the solar wind interacts with the Earth's magnetosphere due to the presence of the planet's intrinsic dipolar magnetic field. In contrast, on Venus, lacking a significant magnetic field, the solar wind interacts directly with the ionosphere. In the present context, Mars is an interesting candidate in the solar system as it possesses a localized crustal magnetic field which results in both magnetized and unmagnetized magnetospheres or acts as a hybrid magnetosphere (Acuna et al., 1999; Fowler et al., 2024).

During the period 26-28 December 2022, the Mars Atmosphere and Volatile Evolution (MAVEN) spacecraft (Jakosky et al., 2015) observed an extremely low solar wind density stream ($<1 \text{ cm}^{-3}$) for an extended period ($>24 \text{ h}$) at Mars which was first encountered by Earth. This unusual and extended density depletion was also accompanied by very low-velocity solar wind flows ($<250 \text{ km s}^{-1}$) which resulted in depletion in the solar wind dynamic pressure. This caused a dramatic expansion of the Martian magnetosphere and bow shock (Halekas et al., 2023). Estimations suggest that the boundaries of the Martian magnetosphere expanded by thousands of kilometers, surpassing the typical location of the bow shock (Halekas et al., 2023). This remarkable event is famously known as "The Day the Solar Wind Disappeared at Mars" or disappearing solar wind (DSW) (Halekas et al., 2023). A similar type of low-density event was first detected by the Advanced Composition Explorer (ACE) satellite on Earth during 10-12 May 1999 (Lockwood, 2001; Janardhan et al., 2008). Recently, it has been revealed that the origin of such solar wind disappearance events is mostly associated with CIR events (Rout et al., 2023, Shaver et al. 2024). The study of Rout et al., 2023 showed the relation between these low-density events and solar wind non-radial flow and their impact on Earth's magnetosphere. The impact of this event on the Earth's magnetosphere-ionosphere system has also been reported by various studies (Farrugia et al., 2008; Le et al., 2000; Ohtani et al., 2000). However, it is particularly noteworthy to mention the observation of a similar rare event at Mars during a fortuitous MAVEN spacecraft orbit. This unique opportunity enables us to further explore its impact on the Martian ionosphere.

Few studies have delved into the interaction between the solar wind and Mars under tenuous solar wind conditions, as well as its impact on Mars's magnetosphere-ionosphere

system (Fowler et al., 2024; Halekas et al., 2023; Shaver et al., 2024; Xu et al., 2024). Notably, Xu et al. (2024) explored the dynamics of superthermal electrons on Mars during a solar wind disappearance event. During this event, the ionosphere experienced expansion, and the upstream solar wind exhibited the ability to alter the Mars-solar wind interaction state within remarkably short timeframes-less than one MAVEN orbit (~ 3.5 hours) (Fowler et al., 2024). However, no study has yet investigated the impact of this extremely low-density event on ionospheric species and plasma density. Thus, this study, for the first time, reports the effects on ionospheric species for both electrons and ions species, i.e., heavier (NO^+ , O_2^+ , and CO_2^+) and lighter (C^+ , N^+ , O^+ , and OH^+) ions, particularly on the nightside due to the absence of MAVEN observations on the dayside. This event presents a unique opportunity to probe planetary interactions' dynamic and evolving nature amidst tenuous solar wind conditions.

2. Data

The low-density solar wind event was observed by a MAVEN spacecraft on 26-28 December 2022 on Mars. In order to address the variation of Martian ionospheric species during this event, we utilized the datasets from multi-instruments aboard MAVEN for observations of the solar wind, IMF, and Martian plasma variation. During December 2022, the MAVEN spacecraft followed an elliptical orbit of nearly 3.5 hours with an apoapsis and a periapsis around 4500 and 180-190 km altitudes, respectively. The MAVEN periapsis surveils the nightside ionosphere over southern latitudes ($\sim 0\text{-}70^\circ$ S) during this period. In the present study, the sampling of the upstream solar wind and IMF conditions are performed by leveraging the in-situ key parameter datasets of Solar Wind Ion Analyzer (SWIA; Dunn, 2023; Halekas et al., 2015) and Magnetometer (MAG; Connerney, 2015; Dunn, 2023). The SWIA instrument is a cylindrical symmetric electrostatic analyzer that measures ion velocity distribution in the 3-axis and covers a broad energy range of 5-25000 eV. It monitors the plasma in a $360 \times 90^\circ$ field of view with a resolution of $\sim 22.5^\circ$ (Halekas et al., 2015). Measurements of MAG instrument datasets have been used to calculate the resultant interplanetary magnetic field (IMF ($|\mathbf{B}|$)) over the period of observation. The MAVEN MAG instrument is a tri-axial fluxgate magnetometer which measures the ambient vector magnetic field in three dimensions during spacecraft orbit and covers a range of ± 65536 nT. The SWIA and MAG in-situ key parameters datasets were accessed and analyzed using the Python Data Analysis and Visualization tool (PyDIVIDE; MAVEN SDC et al., 2020) and NASA Planetary Data System (PDS).

The measurements of electron density were obtained using the Langmuir Probe and Waves (LPW; Andersson et al., 2015; Dunn, 2023) instrument onboard MAVEN. The LPW

instrument is optimized to probe the electron density falls within the range of 10^2 - 10^6 cm^{-3} . The data is accessed using the PyDIVIDE tool. In addition, the Martian nightside ionospheric species densities data was obtained using a Neutral Gas and Ion Mass Spectrometer (NGIMS; Mahaffy, Benna et al., 2015) aboard MAVEN. The NGIMS instrument is designed to measure the ions and neutrals in the mass range of 2-150 amu with unit resolution and monitors the Martian ionosphere between 125 and 500 km altitude during MAVEN spacecraft periapsis. The NGIMS dataset was accessed using the MAVEN science data center and NASA PDS. The information related to different levels and versions of the datasets associated with SWIA, MAG, LPW, and NGIMS instruments is provided in the data availability section below.

3. Results

On 26 December 2022, an extremely low-density solar wind was observed (Halekas et al., 2023) on Mars. This event was described as a disappearing solar wind event (DSW) (Xu et al., 2024; Shaver et al., 2024). In order to investigate the Martian ionospheric response to this low-density solar wind event, we have explored the topside ionosphere in the nightside. The following sub-sections show the results on the variation of solar wind and the Martian ionospheric species during the DSW event in comparison to the pre- and post-event periods.

3.1 Observations of solar wind and IMF on Mars from 15-31 December 2022 using SWIA and MAG datasets onboard MAVEN

Fig. 1 depicts the upstream solar wind plasma and IMF observations between 15 and 31 December 2022. For the pristine solar wind measurements, we leverage the advantage of the Halekas et al. (2017) algorithm above 4400 km altitude from Mars surface. The y -axis for each panel (Fig. 1) from top to bottom (a-d) represents the solar wind density, velocity, solar wind dynamic pressure (SWDP), and resultant IMF ($|B|$) variation with respect to the respective days of December 2022 on the x -axis. The observations of solar wind and IMF indicate a corotating interaction region (CIR) event that started on 21 December and finally ended on 25 December with maximum enhancement in velocity (for more detail, see Shaver et al., 2024). The CIR passage is followed by a rarefaction region with very low solar wind density from 26-28 December 2022. In order to find the Martian ionospheric response during this extremely low solar wind density event, we have analyzed the Martian ionospheric species variation for pre-, post-, and during the DSW event. We selected the pre- and post-event datasets outside the CIR to provide a quiet background scenario, enabling a better comparison with DSW event. The vertical dotted lines illustrate MAVEN orbits during the pre-event (black color), DSW event (red color), and post-event (magenta color). The vertically dotted colored lines indicate

the Martian ionospheric species profile variation that is illustrated with similar color scheme in the next section. During the DSW event, the solar wind density and dynamic pressure almost disappeared and approached nearly 0.15 cm^{-3} and 0.014 nPa , respectively (Fig. 1a&c). Panel b shows the decline in the solar wind velocity during DSW with the lowest magnitude approaching nearly 228 km s^{-1} . The resultant IMF ($|\mathbf{B}|$) during this period lies near to 7 nT (Fig. 1d). Due to MAVEN spacecraft trajectory constraints and elliptical orbit (Jakosky et al., 2015), it does not take the upstream solar wind and ionosphere measurements simultaneously and having a difference of a few hours. All selected profiles (shown by vertically dotted colored lines) during DSW and pre- & post-event periods fell within the similar SZA ($\sim 120\text{-}170^\circ$) range.

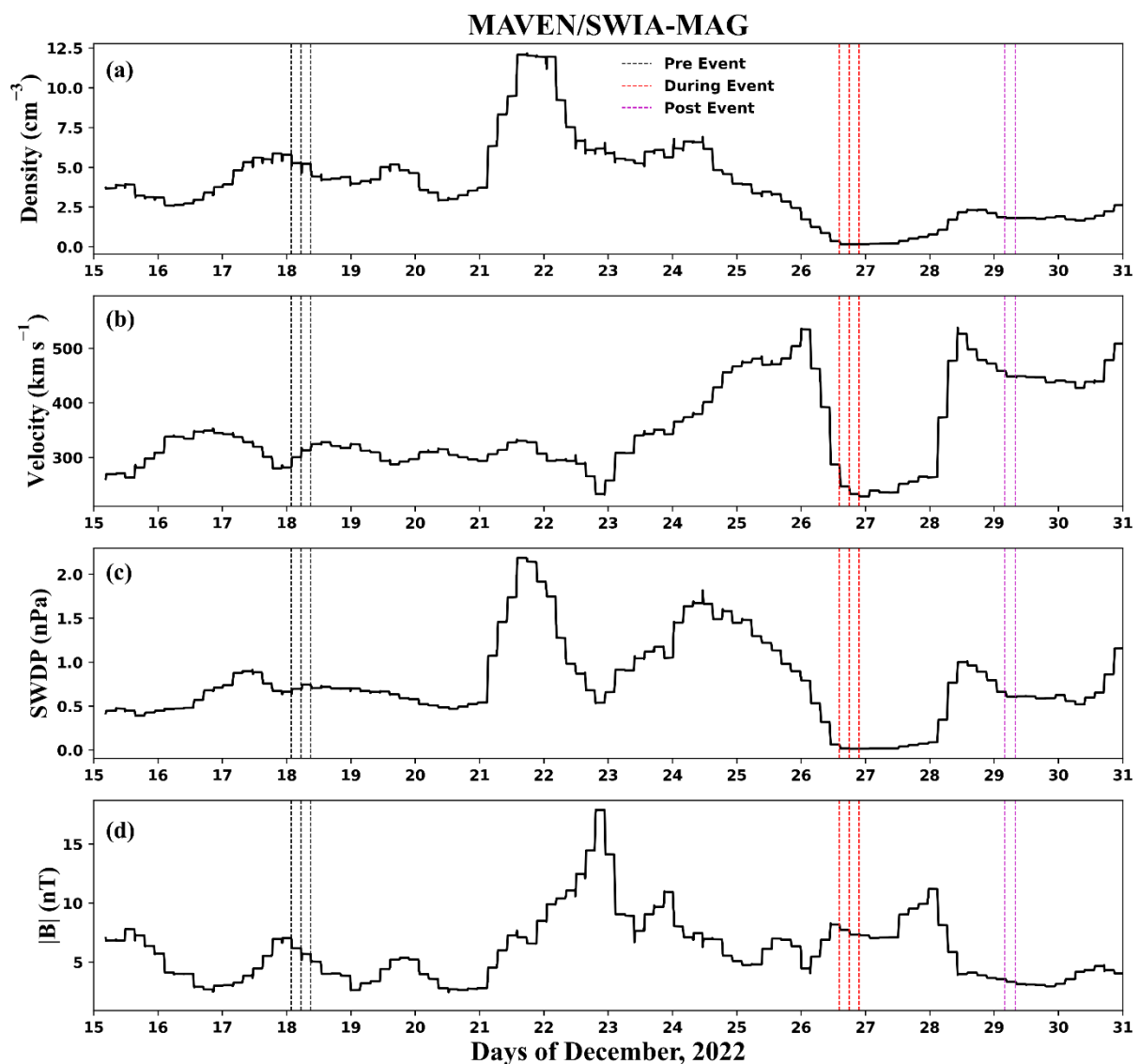


Fig. 1. The MAVEN/SWIA-MAG Observations of the solar wind (a-d) density, velocity, dynamic pressure, and IMF ($|\mathbf{B}|$) respectively near Mars, during December 2022.

3.2 Martian nightside ionosphere during solar wind disappearance event on 26 December 2022

In order to address the DSW event's impact on the Martian topside ionosphere, we have utilized the LPW and NGIMS measurements onboard the MAVEN spacecraft. The MAVEN spacecraft measures the Martian ionospheric composition during its periapsis (Andersson et al., 2015; Benna et al., 2015; Jakosky et al., 2015). During December 2022, the MAVEN periapsis inbound phase, monitors the ionospheric compositions primarily on the nightside of Mars' southern latitudes. However, during the MAVEN outbound leg, the dayside measurements are falling at higher altitudes with different SZA, primarily deprived of ionospheric data and cannot be utilized for the ionospheric study. Therefore, in the present work, we have primarily presented and focused on the behavior of the Martian nightside ionosphere in response to the DSW event.

Fig. 2. represents the LPW and NGIMS in-situ measurements for electron and ion density as a function of altitude. A similar color scheme has been followed as shown in Fig. 1 for pre- and post-event profiles. These profiles were calculated by averaging a 7 km altitude bin of density (shown by black, red, and magenta colors in Fig. 2 and at least 2-3 profiles with similar SZA range have considered). Due to the unavailability of electron and ion density full altitude profiles data for 27 December 2022, we have shown here the average ionospheric profile with standard deviation bar (red color) on 26 December 2022 (red dotted vertical lines in Fig. 1) during the DSW event on Mars. The top panel of Fig. 2 represents the variation of the electron and heavier ions (NO^+ , O_2^+ , and CO_2^+). In contrast, the bottom panel represents the variation of lighter ions (C^+ , N^+ , O^+ , and OH^+) with respect to the altitude. Fig. 2 shows a noticeable change in the magnitude of electrons, heavier, and lighter ions density during the DSW event compared to the pre- and post-event. During the DSW event (red color), the electron density (Fig. 2a) enhanced below 280 km altitudes with maximum magnitude occurring at ~ 250 km altitude compared to pre-event (black color). The post-event period (magenta color) shows that the electron density profiles seem to return to its background condition. During the DSW event, the increased electron density around 250 km is ~ 2.5 times larger than average quiet time magnitude. Similarly, for heavier and lighter ions (Fig. 2b-h), we have observed larger magnitude density profiles during DSW as compared to pre- and post-event. Further, for the post-event period, the ionosphere retraced to its background condition. During the DSW event, the heavier as well as lighter ions, show the peak enhancement in density at around 235 and 280 km altitudes respectively, whereas for pre-and post-event scenario, the maximum magnitude of density lies in the altitude range of 195-230 km. During

the event, the maximum enhancement in heavier ions i.e., NO^+ , O_2^+ and CO_2^+ densities are 18, 39, and 21 times larger, whereas, for lighter ions i.e., C^+ , N^+ , O^+ , and OH^+ densities are 15, 10, 67, 23 times larger as compared to average quiet time. Furthermore, Fig. 2 also depicts that the variability (as shown by 1σ deviation) of the average altitudinal ion profile during the DSW event is more pronounced (>200 km) as compared to pre- and post-event scenarios. Although, the large standard deviation of pre-and post-event profiles around 180-190 km altitude is primarily due to MAVEN maneuvering from periapsis inbound to outbound phase by altering spacecraft orientation. In totality, during the DSW event, the increase in the magnitude of density is quite similar for both heavier and lighter ions in the topside ionosphere (>200 km). Hence, the comparative analyses between DSW and pre- & post-event periods indicate the expansion of the Martian nightside ionosphere during the DSW event as compared to the pre- and post-event periods. For brevity, the detailed information related to the maximum magnitude of electron and ion density with respect to altitude during pre-, DSW, and post-event has been listed in Table 1.

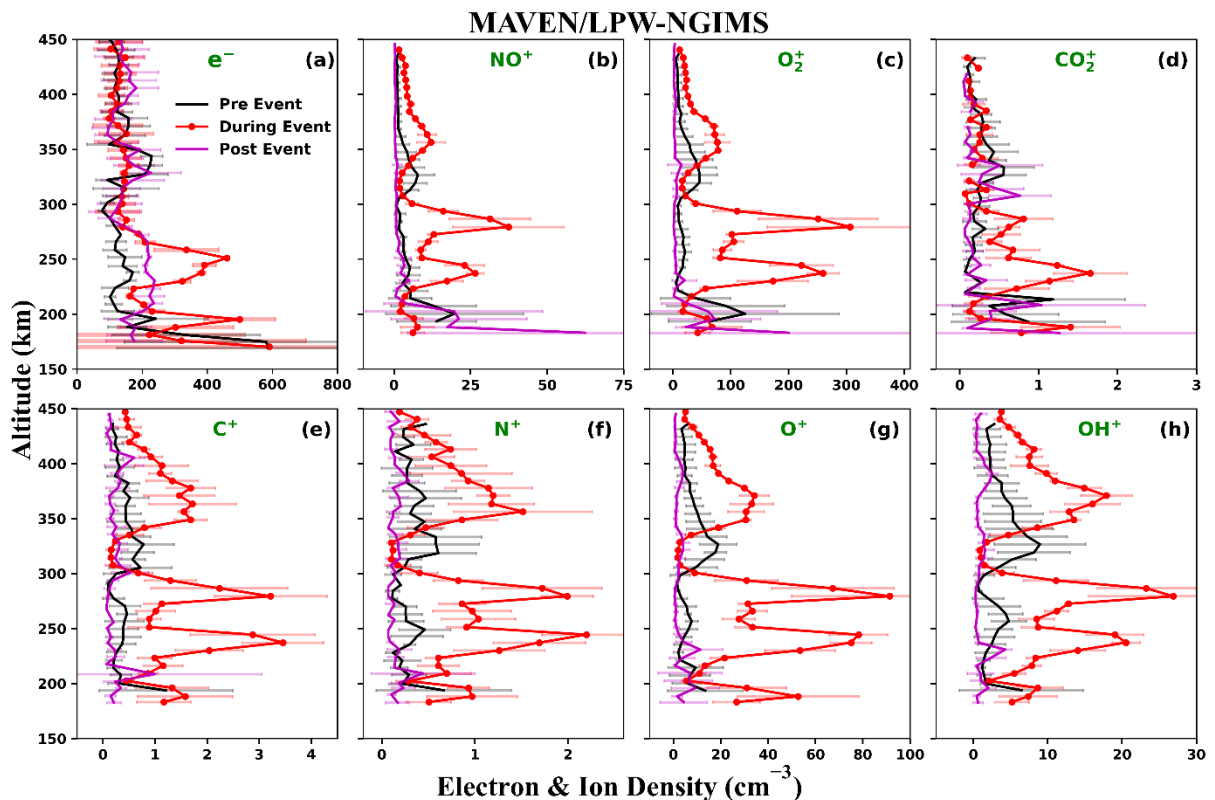


Fig. 2. The Langmuir Probe & Wave (LPW) and Neutral Gas and Ion Mass Spectrometer (NGIMS), observations during MAVEN periapsis orbit, for average (a) electron and (b-h) ions density profiles with standard deviation in the Martian nightside ionosphere as a function of altitude (150–450 km) during 26 December 2022 (red color), along with pre- and post-event (black & magenta colors) period average profiles.

Table 1

The maximum (max.) average magnitude of electron and ions (NO^+ , O_2^+ , CO_2^+ , C^+ , N^+ , O^+ , and OH^+) densities in the Martian nightside ionosphere during the pre-, DSW, and post-event periods. The abbreviations (Dens., and Alt.) used here represent the maximum density and altitude, respectively.

Species	$[\text{e}^-]_{\text{max.}}$		$[\text{NO}^+]_{\text{max.}}$		$[\text{O}_2^+]_{\text{max.}}$		$[\text{CO}_2^+]_{\text{max.}}$		$[\text{C}^+]_{\text{max.}}$		$[\text{N}^+]_{\text{max.}}$		$[\text{O}^+]_{\text{max.}}$		$[\text{OH}^+]_{\text{max.}}$	
	Alt. (km)	Dens. (cm^{-3})	Alt. (km)	Dens. (cm^{-3})	Alt. (km)	Dens. (cm^{-3})	Alt. (km)	Dens. (cm^{-3})	Alt. (km)	Dens. (cm^{-3})	Alt. (km)	Dens. (cm^{-3})	Alt. (km)	Dens. (cm^{-3})	Alt. (km)	Dens. (cm^{-3})
Pre-Event	200	210	200	19.7	200	125	215	1.18	195	1.21	195	0.67	195	13.5	195	6.5
DSW-Event	250	461	235 280	26.5 37.4	235 280	260 306	235	1.7	235 280	3.5 3.2	245 280	2.2 2.0	245 280	78.2 91.3	235 280	20.5 27
Post-Event	200	222	195	21	185	199	210	1.04	205	1.0	195	0.23	195	9.2	195	5.0

4. Discussion and Conclusions

The present study shows how the electron and ion densities change in the Martian nightside ionosphere during the solar wind disappearance event and provides an end-member case of the Mars-solar wind interaction. The key finding is that the Martian nightside electron and ion densities are enhanced with a magnitude larger than 2.5 and 10-67 times, respectively, compared to the average quiet time (Fig. 2). Usually, the nightside peak electron density occurs between 120-180 km altitudes (Haider et al., 1992; Lillis et al., 2009), whereas for lighter and heavier ions, it ranging between 180-200 and 140-160 km altitudes, respectively (Fox et al., 1993; Haider et al., 1997; Girazian et al., 2017). These altitudes are near or below the MAVEN periapsis and cannot be observed in the in-situ measurements by LPW and NGIMS instruments. Above these altitudes, the ionospheric density decreases exponentially. However, our analyses suggest that during the DSW event, the plasma density increases at the top side of the ionosphere.

The previous studies found a prominent depletion in the Martian nightside ionospheric compositions during the periods of high dynamic pressure and IMF (ICMEs and CIRs) (Girazian et al., 2019; Krishnaprasad et al., 2019; Ram et al., 2023, 2024; Thampi et al., 2021). In contrast, during extremely low density and dynamic pressure (DSW) event, the recent work by Halekas et al. (2023) and Shaver et al. (2024) found that magnetospheric-ionospheric boundaries expanded by thousands of kilometers on the dayside and a transition of the

terminator ionosphere from a magnetized to an unmagnetized state. In our study, the pronounced increment of electron and ion density at higher altitudes during DSW indicates the ionospheric expansion from the lower (near MAVEN periapsis or below) to the top nightside ionosphere. The ionospheric expansion primarily depends on the pressure balance between the solar wind dynamic pressure and the thermal pressure of the ionosphere (Nagy, 2004; Sánchez-Cano et al., 2021). During the DSW event, the solar wind dynamic pressure ($\sim 1.4 \times 10^{-11}$ nPa; Fig. 1c of this manuscript) is found to be nearly one order lesser in magnitude in comparison to the nightside ionospheric thermal pressure ($\sim 10^{-10}$ nPa; Halekas et al., 2023 (Fig. 7)). In response to this unbalanced state or to stabilize, there is an extension in the nightside ionosphere from low to higher altitudes, causes larger electron and ion density at higher altitudes (Flynn et al., 2017). Secondly, the expanded dayside magnetosphere-ionosphere to a higher altitude during the DSW event (as demonstrated by Fowler et al. (2024) and Halekas et al. (2023)) can also drive day-to-night plasma cross-terminator transport via crustal magnetic field lines (Adams et al., 2018; Craven et al., 1982; Girazian et al., 2017; Xu et al., 2016, 2017) and may seed the nightside ionosphere at higher altitudes (Cui et al., 2015; Girazian et al., 2017; González-Galindo et al., 2013; Qin et al., 2022).

In order to depict the overall scenario of the Martian ionosphere for pre-, during, and post-DSW event periods, a schematic diagram is provided in Fig. 3. The top panel (Fig. 3a) shows the location of bow shock (dotted black line), the size of the magnetosphere (dotted green line) and ionosphere (brown shades) of Mars during normal solar wind conditions. The ionospheric plasma density (shown by black and magenta-colored dotted curves, respectively; see legends) during pre- and post-event times are also marked. Figure 3b illustrates the impact of the DSW event on the location of bow shock, and the size of the magnetosphere-ionosphere system. The arrow mark indicates how the plasma gets transported from dayside to nightside through magnetic field lines. This simple schematic diagram vividly portrays the expansion of bow shock, magnetosphere, and particularly the Martian ionosphere which is evident from Figure 2. The extent and shape of the terrestrial magnetosphere mainly depend on the solar wind conditions particularly wind dynamic pressure (Ingale et al., 2019, Halekas et al., 2023; Sánchez-Cano et al., 2021). The location of these plasma boundaries is found to be significantly affected during the DSW event due to extremely low solar wind dynamic pressure. In addition to solar wind dynamic pressure, IMF, and cross-terminator plasma transport can also significantly alter the Martian nightside top ionosphere (Girazian et al., 2019; Sakai et al., 2021), resulting in heightened ionospheric density during DSW event.

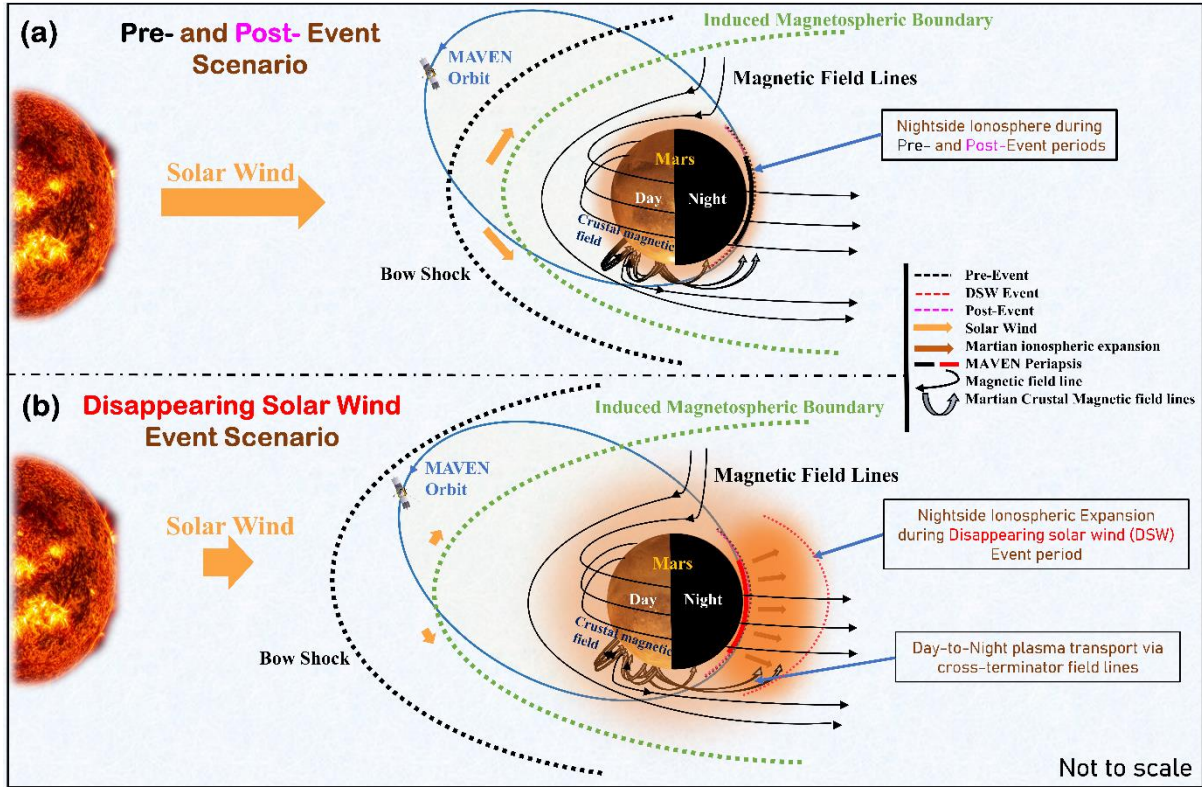


Fig. 3. A schematic that portrays the Mars-solar wind interaction. The top panel depicts the Martian ionosphere during pre- and post-event periods, whereas, the bottom panel represents the solar wind disappearance period (26 December 2022). The schematic is not drawn to scale.

In conclusion, we have found a denser nightside ionosphere during DSW event, where plasma density increases by a factor of ~ 2.5 (for electron) and $10-67$ (for ions) compared to the average quiet time. The increased plasma density at a fixed altitude suggests an expansion of nightside ionosphere (Qin et al., 2022). Thus, this study deepens our understanding of an unusual Mars-solar wind interaction phenomenon and further advances us to study the Mars-like planetary/exoplanetary bodies having magnetized/non-magnetized or hybrid-magnetosphere. In addition, this study provides significant implications for future spacecraft orbit adjustments in the ionospheric region, especially during the periods when the solar wind nearly disappears around the planet. Moreover, this study can help us to comprehend the space weather impact of these events on the planetary atmosphere while quantifying the baseline conditions of the magnetosphere and ionosphere system.

5. Data Availability

The MAVEN dataset utilized during this work are accessible through the NASA Planetary Data System at <https://pds-ppi.igpp.ucla.edu/search/?t=Mars&sc=MAVEN&facet=SPACECRACKT>

_ NAME&depth=1 and MAVEN SDC (<https://lasp.colorado.edu/maven/sdc/public/>). The MAVEN in-situ datasets using LPW Level 2, version_19, revision_01 (Andersson et al., 2017; Dunn et al., 2023), NGIMS (ions density) Level 2, version_08, revision_01 (Benna & Lyness, 2014), SWIA (solar wind ion) Level 2, version_19, revision_01 (Dunn et al., 2023; Halekas, 2017), and MAG (IMF) Level 2, version_19, revision_01 (Connerney, 2017; Dunn et al., 2023) data product bundles utilized during this work are accessed from the NASA Planetary Data System (PDS) and can directly be downloaded using the Python Data Analysis and Visualization tool (MAVEN SDC et al., 2020).

6. Acknowledgement

We sincerely acknowledge the NASA PDS and MAVEN team for the datasets. L. Ram acknowledges the fellowship from the Ministry of Education, Government of India for carrying out this research work. This work is also supported by the Department of Space and the Ministry of Education, Government of India.

References

- Acuna, M., Connerney, J., Ness, Lin, R., Mitchell, D., Carlson, C., et al. (1999). Global distribution of crustal magnetization discovered by the Mars Global Surveyor MAG/ER experiment. *Science*, 284(5415), 790-793. <https://doi.org/10.1126/science.284.5415.790>
- Adams, D., Xu, S., Mitchell, D. L., Lillis, R. J., Fillingim, M., Andersson, L., et al. (2018). Using magnetic topology to probe the sources of Mars' nightside ionosphere. *Geophysical Research Letters*, 45(22), 12-190. <https://doi.org/10.1029/2018GL080629>
- Andersson, L. (2017). MAVEN Langmuir Probe and Waves (LPW) bundle [Dataset]. *NASA Planetary Data System*. <https://doi.org/10.17189/1410658>
- Andersson, L., Ergun, R. E., Delory, G. T., Eriksson, A., Westfall, J., Reed, H., et al. (2015). The Langmuir Probe and Waves (LPW) instrument for MAVEN. *Space Science Reviews*, 195(1-4), 173-198. <https://doi.org/10.1007/s11214-015-0194-3>
- Benna, M., & Lyness, E. (2014). MAVEN neutral gas and ion mass spectrometer data [Dataset]. *NASA Planetary Data System*. <https://doi.org/10.17189/1518931>
- Benna, M., Mahaffy, P. R., Grebowsky, J. M., Fox, J. L., Yelle, R. V., & Jakosky, B. M. (2015). First measurements of composition and dynamics of the Martian ionosphere by MAVEN's neutral gas and ion mass spectrometer. *Geophysical Research Letters*, 42(21), 8958-8965. <https://doi.org/10.1002/2015GL066146>
- Connerney, J. E. (2017). MAVEN magnetometer (MAG) calibrated data bundle [Dataset]. *NASA Planetary Data System*. <https://doi.org/10.17189/1414178>
- Connerney, J. E., Espley, J. R., Lawton, P., Murphy, S., Odom, J., Oliverson, R., & Sheppard, D. (2015). The MAVEN magnetic field investigation. *Space Science Reviews*, 195(1), 257-291. <https://doi.org/10.1007/s11214-015-0169-4>
- Connerney, J. E. P., Acuña, M. H., Wasilewski, P. J., Kletetschka, G., Ness, N. F., Reme, H., et al. (2001). The global magnetic field of Mars and implications for crustal evolution. *Geophysical Research Letters*, 28(21), 4015-4018.
- Cravens, T. E., Brace, L. H., Taylor, H. A., Jr., Russell, C. T., Knudsen, W. L., Miller, K. L., et al. (1982). Disappearing ionospheres on the nightside of Venus. *Icarus*, 51(2), 271-282. [https://doi.org/10.1016/0019-1035\(82\)90083-5](https://doi.org/10.1016/0019-1035(82)90083-5)
- Cui, J., M. Galand, R. V. Yelle, Y. Wei, and S.-J. Zhang (2015), Day-to-night transport in the Martian ionosphere: Implications from total electron content measurements, *Journal of Geophysical Research: Space Physics*, 120, 2333-2346, doi:10.1002/2014JA020788
- Dunn, P.A., 2023. MAVEN In situ Key Parameters Data Bundle [Dataset]. *NASA Planetary Data System*. <https://doi.org/10.17189/1414174>
- Farrugia, C. J., Gratton, F. T., Jordanova, V. K., Matsui, H., Mühlbachler, S., Torbert, R. B., et al. (2008). Tenuous solar winds: Insights on solar wind-magnetosphere interactions. *Journal of Atmospheric and Solar-Terrestrial Physics*, 70(2-4), 371-376. <https://doi.org/10.1016/j.jastp.2007.08.032>
- Flynn, C. L., Vogt, M. F., Withers, P., Andersson, L., England, S., & Liu, G. (2017). MAVEN observations of the effects of crustal magnetic fields on electron density and temperature in the Martian dayside ionosphere. *Geophysical Research Letters*, 44, 10, 812-10,821. <https://doi.org/10.1002/2017GL075367>
- Fowler, C. M., Shaver, S., Hanley, K. G., Andersson, L., McFadden, J., Mitchell, D., et al. (2024). Disappearing solar wind at Mars: Changes in the Mars-solar wind interaction. *Journal of Geophysical Research: Space Physics*, 129, e2023JA031910. <https://doi.org/10.1029/2023JA031910>
- Fox, J. L., Brannon, J. F., & Porter, H. S. (1993). Upper limits to the nightside ionosphere of Mars. *Geophysical Research Letters*, 20, 1339-1342. <https://doi.org/10.1029/93GL01349>
- Fränz, M., Dubinin, E., Nielsen, E., Woch, J., Barabash, S., Lundin, R., & Fedorov, A. (2010). Transterminator ion flow in the Martian ionosphere. *Planetary and Space Science*, 58(11), 1442-1454. <https://doi.org/10.1016/j.pss.2010.06.009>
- Girazian, Z., Halekas, J., Morgan, D. D., Kopf, A. J., Gurnett, D. A., & Chu, F. (2019). The effects of solar wind dynamic pressure on the structure of the topside ionosphere of Mars. *Geophysical Research Letters*, 46(15), 8652-8662. <https://doi.org/10.1029/2019GL083643>

- Girazian, Z., Mahaffy, P., Lillis, R. J., Benna, M., Elrod, M., Fowler, C. M., & Mitchell, D. L. (2017). Ion densities in the nightside ionosphere of Mars: Effects of electron impact ionization. *Geophysical Research Letters*, *44*(22), 11–248. <https://doi.org/10.1002/2017gl075431>
- González-Galindo, F., J.-Y. Chaufray, M. A. López-Valverde, G. Gilli, F. Forget, F. Leblanc, R. Modolo, S. Hess, and M. Yagi (2013), Three-dimensional Martian ionosphere model: I. The photochemical ionosphere below 180 km, *Journal of Geophysical Research*, *118*, 2105–2123. doi:10.1002/jgre.20150
- Haider, S. A., Kim, J., Nagy, A. F., Keller, C. N., Verigin, M. I., Gringauz, K. I., et al. (1992). Calculated ionization rates, ion densities, and airglow emission rates due to precipitating electrons in the nightside ionosphere of Mars. *Journal of Geophysical Research*, *97*, 10,637–10,641. <https://doi.org/10.1029/92JA00317>
- Haider, S. A. (1997). Chemistry of the nightside ionosphere of Mars. *Journal of Geophysical Research*, *102*, 407–416. <https://doi.org/10.1029/96JA02353>
- Halekas, J. (2017). MAVEN solar wind ion analyzer (SWIA) calibrated data bundle [Dataset]. *NASA Planetary Data System*. <https://doi.org/10.17189/1414182>
- Halekas, J. S., Ruhunusiri, S., Harada, Y., Collinson, G., Mitchell, D. L., Mazelle, C., et al. (2017). Structure, dynamics, and seasonal variability of the Mars-solar wind interaction: MAVEN solar wind ion analyzer in-flight performance and science results. *Journal of Geophysical Research: Space Physics*, *122*(1), 547–578. <https://doi.org/10.1002/2016JA023167>
- Halekas, J. S., Shaver, S., Azari, A. R., Fowler, C. M., Ma, Y., Xu, S., et al. (2023). The day the solar wind disappeared at Mars. *Journal of Geophysical Research: Space Physics*, *128*, e2023JA031935. <https://doi.org/10.1029/2023JA031935>
- Halekas, J. S., Taylor, E. R., Dalton, G., Johnson, G., Curtis, D. W., McFadden, J. P., et al. (2015). The solar wind ion analyzer for MAVEN. *Space Science Reviews*, *195*(1), 125–151. <https://doi.org/10.1007/s11214-013-0029-z>
- Jakosky, B. M., Lin, R. P., Grebowsky, J. M., Luhmann, J. G., Mitchell, D. F., Beutelschies, G., et al. (2015). The Mars atmosphere and volatile evolution (MAVEN) mission. *Space Science Reviews*, *195*, 3–48. <https://doi.org/10.1007/s11214-015-0139-x>
- Janardhan, P., Tripathi, D., & Mason, H. E. (2008). The solar wind disappearance event of 11 May 1999: Source region evolution. *Astronomy and Astrophysics*, *488*(1), L1–L4. <https://doi.org/10.1051/0004-6361:200809667>
- Krishnaprasad, C., Thampi, S. V., & Bhardwaj, A. (2019). On the response of Martian ionosphere to the passage of a corotating interaction region: MAVEN observations. *Journal of Geophysical Research: Space Physics*, *124*(8), 6998–7012. <https://doi.org/10.1029/2019JA026750>
- Le, G., Chi, P. J., Goedecke, W., Russell, C. T., Szabo, A., Petrinc, S. M., et al. (2000). Magnetosphere on May 11, 1999, the day the solar wind almost disappeared: II. Magnetic pulsations in space and on the ground. *Geophysical Research Letters*, *27*(14), 2165–2168. <https://doi.org/10.1029/1999GL000012>
- Lillis, R. J., Fillingim, M. O., Peticolas, L. M., Brain, D. A., Lin, R. P., & Bougher, S. W. (2009). Nightside ionosphere of Mars: Modeling the effects of crustal magnetic fields and electron pitch angle distributions on electron impact ionization. *Journal of Geophysical Research*, *114*, E11009. <https://doi.org/10.1029/2009JE003379>
- Lockwood, M. (2001). The day the solar wind nearly died. *Nature*, *409*, 677–679. <https://doi.org/10.1038/35055654>
- Mahaffy, P. R., Benna, M., King, T., Harpold, D. N., Arvey, R., Barciniak, M., et al. (2015). The neutral gas and ion mass spectrometer on the Mars atmosphere and volatile evolution mission. *Space Science Reviews*, *195*(1), 49–73. <https://doi.org/10.1007/s11214-014-0091-1>
- Maven, S. D. C., Harter, B., Ben, Lucas, E., & Jibarnum (2020). MAVENSDC/Pydivide: First release (version v0.2.13) [Software]. Zenodo. <https://doi.org/10.5281/ZENODO.3601516>
- Nagy, A.F. et al. (2004). The Plasma Environment of Mars. In: Winterhalter, D., Acuña, M., Zakharov, A. (eds) *Mars' Magnetism and Its Interaction with the Solar Wind*. Space Sciences Series of ISSI, vol 18. Springer, Dordrecht. https://doi.org/10.1007/978-0-306-48604-3_2

- Ohtani, S., Newell, P. T., & Takahashi, K. (2000). Dawn-dusk profile of field-aligned currents on May 11, 1999: A familiar pattern driven by an unusual cause. *Geophysical Research Letters*, *27*(23), 3777-3780. <https://doi.org/10.1029/2000GL003789>
- Qin, J., Zou, H., Ye, Y., Hao, Y., & Wang, J. (2022). A denser and elevated Martian nightside ionosphere during Mars season Ls 180–360°. *Icarus*, *388*, 115255. <https://doi.org/10.1016/j.icarus.2022.115255>
- Ram, L., Rout, D., Rathi, R., Mondal, S., Sarkhel, S., & Halekas, J. (2023). A comparison of the impacts of CMEs and CIRs on the Martian dayside and nightside ionospheric species. *Journal of Geophysical Research: Planets*, *128*, e2022JE007649. <https://doi.org/10.1029/2022JE007649>
- Ram, L., Rout, D., Rathi, R., Withers, P., & Sarkhel, S. (2024). Martian M2 peak behavior in the dayside near-terminator ionosphere during interplanetary coronal mass ejections. *Icarus*, *408*, 115857. <https://doi.org/10.1016/j.icarus.2023.115857>
- Rout, D., Chakrabarty, D., Janardhan, P., Sekar, R., Maniya, V., and Pandey, K. (2017). Solar wind flow angle and geoeffectiveness of corotating interaction regions: First results, *Geophysical Research Letters*, *44*, 4532–4539, doi:10.1002/2017GL073038.
- Rout, D., Janardhan, P., Fujiki, K., Chakrabarty, D., & Bisoi, S. K. (2023). The Origin of Extremely Nonradial Solar Wind Outflows. *The Astrophysical Journal*, *950*(1), 1. <https://doi.org/10.3847/1538-4357/acd000>
- Sakai, S., Seki, K., Terada, N., Shinagawa, H., Sakata, R., Tanaka, T., & Ebihara, Y. (2021). Effects of the IMF direction on atmospheric escape from a Mars-like planet under weak intrinsic magnetic field conditions. *Journal of Geophysical Research: Space Physics*, *126*(3), e2020JA028485. <https://doi.org/10.1029/2020JA028485>
- Sánchez-Cano, B., Narvaez, C., Lester, M., Mendillo, M., Mayyasi, M., Holmstrom, M., et al. (2020). Mars ionopause: A matter of pressures. *Journal of Geophysical Research: Space Physics*, *125*(9), e2020JA028145. <https://doi.org/10.1029/2020JA028145>
- Shaver, S. R., Solt, L., Andersson, L., Halekas, J., Jian, L., da Silva, D. E., et al. (2024). The Martian ionospheric response to the co-rotating interaction region that caused the disappearing solar wind event at Mars. *Journal of Geophysical Research: Space Physics*, *129*, e2023JA032181. <https://doi.org/10.1029/2023JA032181>
- Thampi, S. V., Krishnaprasad, C., Nampoothiri, G. G., & Pant, T. K. (2021). The impact of a stealth CME on the Martian topside ionosphere. *Monthly Notices of the Royal Astronomical Society*, *503*(1), 625–632. <https://doi.org/10.1093/mnras/stab494>
- Ulusen, D., and Linscott, I. R. (2008). Low-energy electron current in the Martian tail due to reconnection of draped interplanetary magnetic field and crustal magnetic fields, *Journal of Geophysical Research*, *113*, E06001. doi:10.1029/2007JE002916
- Xu, S., D. Mitchell, C. Dong, S. Bougher, M. Fillingim, R. Lillis, J. McFadden, C. Mazelle, J. Connerney, and B. Jakosky (2016). Deep nightside photoelectron observations by MAVEN SWEA: Implications for Martian Northern Hemispheric magnetic topology and nightside ionosphere source, *Geophysical Research Letters*, *43*, 8876–8884. doi:10.1002/2016GL070527
- Xu, S., Mitchell, D. L., Halekas, J., Brain, D. A., Weber, T., Andersson, L., et al. (2024). Superthermal electron observations at Mars during the December 2022 disappearing solar wind event. *Journal of Geophysical Research: Space Physics*, *129*, e2023JA032258. <https://doi.org/10.1029/2023JA032258>
- Xu, S., Weber, T., Mitchell, D. L., Brain, D. A., Mazelle, C., DiBraccio, G. A., & Espley, J. (2019). A technique to infer magnetictopology at Mars and its application to the terminator region. *Journal of Geophysical Research: Space Physics*, *124*, 1823-1842. <https://doi.org/10.1029/2018JA026366>